Structure and Dielectric Saturation of Water in Hydrated Polymer Electrolyte Membranes: Inclusion of the Internal Field Energy

Reginald Paul*

Department of Chemistry, The University of Calgary, Calgary, Alberta, Canada T2N 1N4

Stephen J. Paddison*,†

Molecular Physics and Theoretical Chemistry Group, Los Alamos National Laboratory, Los Alamos, New Mexico 87545

Received: April 5, 2004; In Final Form: June 10, 2004

The nature of the water in hydrated polymer electrolyte membranes (PEMs) is distinct from that of bulk water and affects the rate of diffusion of protons in the material. Traditional methods used in the study of the phenomenon of dielectric saturation involve the assumption of the presence of a homogeneous or slowly varying external field, conditions that are hardly appropriate for PEMs. If the condition of field homogeneity is relaxed, a nonphysical divergence in the permittivity results. In this paper we show that through proper inclusion of the internal field energy the difficulty is rectified. Our recently derived equilibrium statistical mechanical model for the calculation of the spatial variation in the permittivity of water within PEMs has been extended to include the field energy. Using simple model calculations, we demonstrate that the interaction of the water molecules with the anionic sites constitute a more important contribution to the energy than the intermolecular forces. We have recalculated pore-radial profiles of the dielectric constant of the water in Nafion and 65% sulfonated PEEKK (poly arylene ether ketone) polymer electrolyte membranes over a range of hydration levels obtaining qualitative agreement with experiments. These profiles quantitatively show the increased ordering of the water in the neighborhood of the anionic sites, and although only the affect due to these sites is specifically computed, confinement effects on the water is implicitly included. In separate investigations, it was determined that both the uniformity in the distribution of the sulfonate groups, and the intrusion of these groups into the pore volume, will dramatically affect the permittivity of the water. Together our results help to elucidate the impact of structure and ordering of the water due to the effect of the fixed anionic groups on the underlying mechanisms of proton conduction in PEMs.

Introduction

The fuel cell is a highly efficient device that electrochemically converts energy from renewable sources with practically no pollutant emissions. Among the various types of fuel cells currently under investigation, the polymer electrolyte membrane (i.e., PEM) fuel cell is the choice of most of the automotive industries due to its high power density (i.e., low weight) and low relative (when compared to Solid Oxide Fuel Cells, i.e., SOFCs) cost, and possible use of air as the oxidant. Significant materials research and development must take place, however, to make the fuel cell both technically and economically competitive and viable in stationary and mobile applications.[1]

In a PEM fuel cell, an electrical current is produced through the catalyzed (i.e., Pt or Pt/Ru alloy) oxidation of a fuel (e.g., H_2(g), CH_3OH(aq) etc.) at the anode producing protons, which are transported and consumed through a reductive reaction with oxygen at the cathode, forming water. The PEM functions in the important capacity as the electrolyte medium for proton transport and as the separator of both the electrodes and the fuel and oxygen. Although the past decade has witnessed a dedicated research effort to improve fuel cell catalysts and optimize stack design and operating conditions, the development of a PEM possessing (a) mechanical stability, (b) both thermal stability and high proton conductivity at operating temperatures above 100 °C, (c) impermeability to the fuel (particularly methanol), and (d) acceptable (i.e., 'low') manufacturing costs, remains an elusive but substantially important research goal.[2]

Among the PEMs currently available, Nafion (a DuPont registered trademark perfluorinated sulfonic acid polymer) and the various sulfonated polyetherketones (i.e., PEEK, PEEKK, etc.) have been subject to considerable characterization and testing for fuel cell applications. Reviews of the experimental and theoretical work with these and other membranes have recently been conducted by Doyle and Rajendran,[3] Kreuer,[4] and Paddison.[5,6] Although Nafion has been the prototypical PEM, its high manufacturing cost and permeability to methanol limit the practical utilization in commercial fuel cells. In addition, both the perfluorinated and aromatic membranes are restricted to operating temperature below 90 °C due to insufficient proton conductivity under low humidity conditions. When hydrated, these membranes exhibit a nanophase-separated morphology with the hydrophobic backbone of the polymer separated from a network of water and ions (both fixed SO_3^- groups and

* Correspondence may be addressed to either author. E-mail: rpaul@ucalgary.ca or paddison@t12.lanl.gov.

† Now at Department of Chemistry, University of Alabama in Huntsville, Huntsville, Alabama 35899. E-mail: paddison@matsci.uah.edu.

10.1021/jp048501k CCC: $27.50
Published on Web 08/06/2004

hydrated protons).[7] The rigidity of the backbone and the crystallinity of the polymer confine the water; and with the significant density and distribution of the pendant anionic groups give structural ordering to the water in the membrane. Thus, it is in an aqueous medium quite different to bulk water where conduction of protons occurs.

Both experimental[8−11] and molecular dynamics simulations[12−15] have revealed that water confined in systems such as reverse micelles and biological pores possesses a decreased polarity and rate of relaxation, and an increased degree of spatial and orientational order when compared to bulk water. As structural diffusion (i.e., the Grotthuss mechanism) of protons in bulk water require coordinated formation and cleavage of hydrogen bonds of water molecules in the second hydration shell of the hydrated proton (Zundel and Eigen ions),[16−18] any constraint to the dynamics of the water molecules will decrease the mobility of the protons. Thus, knowledge of the state or nature of the water in the membrane is critical to understanding the mechanisms of proton transfer and transport in PEMs.[19−22]

Recently, in an attempt to understand the relationships between the nature of the water in a PEM and its degree of hydration, Paddison et al.[23,24] measured the entire microwave region (0.045−30 GHz) of the dielectric spectrum of both Nafion and PEEK membranes. The choice to conduct measurements at field frequencies up to 30 GHz was based on the observation that the principal absorption band, attributed to a Debye type relaxation of molecular origin, in pure bulk water occurs at about 18 GHz. In addition to obtaining the dielectric constant of these membranes as a function of both water content and frequency (the latter being a difficult quantity to obtain over such a broad range), they also computed conductivities; the latter showing good agreement to the measurements made by others. Their results showed a strong dependence in the dielectric constant and loss factor in the Nafion membranes with water content, but a much weaker dependence in the PEEK membranes. These results are completely consistent with the morphologies derived by Kreuer[7] from SAXS and (PFG) NMR experiments, where due to the stronger confinement of water in the narrow channels of the PEEK membranes the dielectric constant is lower (i.e., the water molecules are more tightly bound − to each other and to the fixed sulfonate groups). Similar conclusions where also reached by MacMillan et al.[25] in proton and deuterium NMR measurements of hydrated Nafion where the reorientational correlation times of the water where found to scale as a function of the pore diameter.

The drawback or limitation, however, in any of these experimental measurements is that the results reflect only the dielectric response of the bulk material (i.e., both the polymer and the water); and thus specific information concerning only the water in the pores is somewhat obscured. An understanding of the dielectric saturation is these nanophase-separated materials will provide critical insight into both the shielding of the anionic fixed groups and the degree of separation of the protons from the conjugate anions. It, therefore, becomes essential that some theoretical work is needed to supplement this experimental work. This is particularly crucial because the membrane pores contain sources of strong electrical fields that substantially alter the physical properties from those predicted by bulk measurements.

From a historical perspective, Böttcher[26] first observed that, contrary to what had been assumed, the permittivity of some substances shows a significant dependence on the magnitude of the field. This implied that the response of a dielectric body to the combination of two electric fields is not equal to the sum of the individual responses to each field acting separately. An example of this coupling is found in the Kerr effect,[27] in which insulating liquids, containing anisotropic molecules, become doubly refracting when subjected to strong fields. The experimental work of Böttcher showed that in analogy with paramagnetism, the phenomenon of a nonlinear response of some substances to the applied field might be referred to as "dielectric saturation". In a purely electrostatic approach to the problem, Coffey and Scaife[28] considered a dielectric sphere in a uniform electric field and solved the Laplace equation both within and outside the sphere introducing the nonlinear aspects of the problem through boundary conditions. Paddison, Paul and Kaler[29] used a similar approach to model the frequency dependent hysteresis loops that are observed in the dielectrophoresis of living plant protoplasts. From a molecular standpoint, Kirkwood[30,31] and Fröhlich[32,33] independently developed the requisite statistical mechanical machinery for the calculation of the permittivity of matter. In Fröhlich's approach the average dipole moment is expressed as a power series in the external field and then the permittivity computed by retaining only the linear term (*linear response theory*). Buckingham[34] included the quadratic term in Fröhlich's expansion and thereby introduced the possibilities of theoretically analyzing dielectric saturation. Booth[35] provided a general expression for computing the dielectric saturation of a collection of hydrogen-bonded dipoles in a *constant* external field. Bontha and Pintauro[36] extended Booth's work, to include inhomogeneous electric fields. Ninhaus and Deutch[37] developed a theory based upon the application of graphical cluster theory to compute the consequences of dielectric saturation in condensed phases. However, the later two formalisms depend on a weak spatial dependence of the field. During recent years fundamental methods have been developed in the context of macromolecules and pore systems. For example Warshel and Papazyan[38] have employed Langevin dipoles to develop models for solvation in biological systems. Sansom, Smith, and Adcock[39] have studied the dynamic response of water in a molecular dynamic simulation of hydrated biological ion channels with a Langevin function.

In prior work on PEMs[36,40,41] it had been assumed that the internal field may be treated as a constant or, at most, a slowly varying function of space. It is necessary to make this assumption to avoid a divergence in the polarization, and thus the permittivity, that arises from the mathematical nature of the Langevin function. The divergence of these two properties becomes very pronounced in regions where the field intensity is high (e.g., in the vicinity of the anionic sites). Such a rise in the permittivity is clearly contrary to the phenomenon of dielectric saturation, where a fall in the permittivity is expected. It is therefore surprising that such an approximation must be made in a theory that is based on rigorous principles to obtain physically acceptable results. This leads one, therefore, to suspect that some quantity has been inadvertently ignored.

A careful examination of the underlying Hamiltonian shows that the energy of the internal field itself has not been included in any of these models. This is an inconsistency, because the kinetic energy of the water molecules is implicitly included, but the internal electrical field energy has been neglected. It should be noted, however, that even though the kinetic energy of the water molecules may be included in the Hamiltonian it does not play any role in the subsequent calculations of the excess Helmholtz free energy. Such is not, however, the case with the energy of the internal field.

Theoretical Model

Basic Equations. The theoretical principles that are needed in the calculation have already been introduced in our earlier

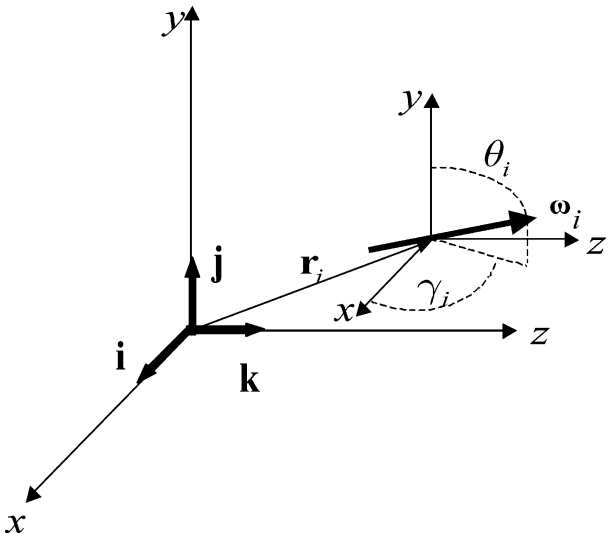

Figure 1. Implemented coordinate scheme used for denoted the position of an arbitrary water molecule (treated as a dipole) whose orientation is specified with a vector ω_i, and located at a position $\mathbf{r}_i$ within the pore.

work[40,41] and therefore only briefly described here to facilitate of the model construct and a description of the notation.

The network of water and ions are confined in nano-dimensioned domains within the membrane (i.e., nanopores) and are modeled as cylinders, to the walls of which are attached the pendant sulfonic acid groups that protrude into the pore interior. As the sulfonic acid groups are very strong acids, even a small amount of absorbed water in the membrane results in substantial ionization. This produces sulfonate groups that are "fixed" or tethered to the polymer backbone and much more mobile hydrated protons (i.e., H_3O^+, $H_5O_2^+$, etc.). Owing to entropy maximization, the protons are present in a relatively more diffuse state than the $-SO_3^-$ ions. As a consequence of this spatial distribution of charges, the electrical field is not homogeneous and will tend to be much stronger in the vicinity of the fixed anionic sites. Thus an individual pore is modeled as a cylinder of length L and radius R.

(1) The starting point of the analysis is the introduction of a suitable classical mechanical Hamiltonian, H. The precise details of this quantity and its appropriate choice will be presented later.

(2) We employ the symbols $\{x\}$ and $\{p\}$ to denote the set of coordinates and conjugate momenta for the complete specification of the phase space of the water molecules. In this notation the element $x_i \in \{x\}$ refers to all the variables that are required to specify the complete position and orientation of the ith water molecule in the pore, and is thus an abbreviation of the form

$$x_i \equiv (\mathbf{r}_i, \omega_i)$$

Here, $\mathbf{r}_i$ is the vector position of the center of mass of the ith molecule and ω_i is a vector, which, in general, depends on the three Euler angles required to specify the orientation of a nonlinear molecule. In the present analysis we assume that the water molecules may be treated as linear molecules with dipole moment μ. As a consequence of this assumption, only two polar angles (θ_i, γ_i) are needed and ω_i may be expressed in terms of the unit Cartesian vectors **i**, **j**, and **k** as

$$\omega_i \equiv \mathbf{i} \sin\theta_i \cos\gamma_i + \mathbf{j} \sin\theta_i \sin\gamma_i + \mathbf{k} \cos\theta_i$$

This notation convention is given in Figure 1. The elements of the set $\{p\}$ are the canonical conjugate momenta. Thus, the element $p_i \in \{\mathbf{p}_i, \mathbf{L}_i\}$ is composed of the linear momentum $\mathbf{p}_i$ of the center of mass of the ith water molecule and the angular momenta $\mathbf{L}_i$ that correspond to each angular rotation.

(3) With the notation described above we introduce the details of the Hamiltonian. This quantity is a sum of the energy of the internal field, U_F, the kinetic energy of the water molecules, T_W, and the total potential energy UN:

$$H = U_F + T + U_N$$

(a) In the present treatment we consider two electrical fields: A *weak* external field to be designated by the symbol $\mathbf{E}_e$ whose origin lies in sources that reside outside the nanopore and an internal field **E** that originates in the cations (H_3O^+) and anions ($-SO_3^-$) within the nanopore, as discussed above. In the more traditional approach the internal field **E** is assumed to play the role of the external field $\mathbf{E}_e$. The mathematical form of the internal field energy is discussed in the appendix. It is evident that if a water molecule with center of mass located at $\mathbf{r}_i$ is removed from the system, then a cavity of volume ϑ will be created. This cavity will contain an amount of energy given by $(\epsilon_0/2)\vartheta E^2(\mathbf{r}_i)$, and therefore the contribution from all the cavities given by eq 29 must be included in the Hamiltonian. Ideally, an energy contribution from the external field should also be included; however, we assume that this is a weak field, making a negligible contribution.

In this paper we use the form of the internal field that has previously been employed in our earlier work and is given by the equation

$$\mathbf{E}(\mathbf{r}) = \frac{2ef_n n^2}{\epsilon_0 L^2}\left[\mathbf{e}_\rho K_1\left\{\frac{2\pi n(R-\rho)}{L}\right\}\cos\left(\frac{2\pi nz}{L}\right) - \mathbf{k}K_0\left\{\frac{2\pi n(R-\rho)}{L}\right\}\sin\left(\frac{2\pi nz_i}{L}\right)\right] \quad (1)$$

In writing such an expression, we assume that the anionic groups are arranged in the form of an array of n negatively charged rings or circular arrays attached to the pore wall; each ring containing f_n anionic sites. The above formula has been presented in a cylindrical coordinate frame (ρ, φ, z) in which the pore axis is placed along the $z$axis; $\mathbf{e}_\rho$ is the unit radial vector with radial coordinate ρ. Because of the axial symmetry of the rings, there is no dependence of the field on the angular variable φ. The functions K_0 and K_1 are respectively the zero and first-order modified Bessel functions. In general, the pendant groups may protrude into the pore interior with a length p. If the protrusion length is included in eq 1, then the quantity $(R-\rho)$, which represents the radial distance of the point of interest (ρ, φ, z) from the pore wall, is replaced by $(R-p-\rho)$.

(b) The kinetic energy contributions from the water molecules are given by

$$T_W = \sum_{i=1}^{N}\frac{p_i^2}{2m} + \sum_{i=1}^{N}\left(\frac{L_{ai}^2}{2I_a} + \frac{L_{bi}^2}{2I_b} + \frac{L_{ci}^2}{2I_c}\right) \quad (2)$$

Here, m is the mass of each water molecule, I_a, I_b, and I_c are the moments of inertia along the principal axes a, b, and c, respectively. Within our approximation of treating the water molecules as rigid linear molecules, the kinetic energy reduces to

$$T_W = \sum_{i=1}^{N} \frac{p_i^2}{2m} + \sum_{i=1}^{N} \frac{1}{2I}\left(L_{\theta i}^2 + \frac{L_{\gamma i}^2}{\sin^2 \theta_i}\right) \quad (3)$$

Here $L_{\theta i}$ and $L_{\gamma i}$ are the angular momenta of the ith molecule for rotation about the polar angles θ_i and γ_i, respectively.

(c) The function $U_N(\{x\},\mathbf{E},\mathbf{E}_e)$ that appears in H is the full N-body potential energy of the fluid within the nanopore. To proceed with the calculations, an appropriate form for U_N must be chosen. We assume that, at least, three potential energy terms make significant contributions: (i) the sum of the pairwise interactions between the water molecules ($U_{WW} = \sum_{i<j}^{N} \psi(x_i,x_j)$); (ii) the interaction between the internal field and all the water molecules ($U_{FW}^{(int)} = -\mu\sum_{i<1}^{N} \omega_i \cdot \mathbf{E}(\mathbf{r}_i)$); and (iii) the analogous term due to the external field ($U_{FW}^{(ext)} = -\mu\sum_{i<1}^{N} \omega_i \cdot \mathbf{E}_e(\mathbf{r}_i)$). Thus, the total potential energy will be given by

$$U_N(\{x\},\mathbf{E},\mathbf{E}_e) = \sum_{i<j}^{N} \psi(x_i,x_j) - \mu\sum_{i=1}^{N} \omega_i \cdot \mathbf{E}(\mathbf{r}_i) - \mu\sum_{i=1}^{N} \omega_i \cdot \mathbf{E}_e(\mathbf{r}_i) \quad (4)$$

The precise form of the function $\psi(x_i,x_j)$ will be presented later.

(4) The total Hamiltonian may now be written as a sum of all the energy terms computed above

$$H(\{p\},\{x\},\mathbf{E},\mathbf{E}_e) = \frac{\epsilon_0}{2}\vartheta\sum_{i=1}^{N} E^2(\mathbf{r}_i) + \sum_{i=1}^{N} \frac{p_i^2}{2m} + \sum_{i=1}^{N} \frac{1}{2I}\left(L_{\theta i}^2 + \frac{L_{\phi i}^2}{\sin^2 \theta_i}\right) + \sum_{i<j}^{N} \psi(x_i,x_j) - \mu\sum_{i=1}^{N} \omega_i \cdot \mathbf{E}(\mathbf{r}_i) - \mu\sum_{i=1}^{N} \omega_i \cdot \mathbf{E}_e(\mathbf{r}_i) \quad (5)$$

At this point we introduce a function $\phi(x_i)$ that includes all the one-body terms in the Hamiltonian that depend only upon the *spatial* variable x_i, i.e.

$$\phi(x_i) \equiv \frac{\epsilon_0}{2}\vartheta E^2(\mathbf{r}_i) - \mu\omega_i \cdot \mathbf{E}(\mathbf{r}_i) - \mu\omega_i \cdot \mathbf{E}_e(\mathbf{r}_i) \quad (6)$$

(5) From the Hamiltonian the canonical partition function $Q(N,V,T,\boldsymbol{E},\mathbf{E}_e)$ can be calculated by using the standard techniques of statistical mechanics:

$$Q(N,V,T,\mathbf{E},\mathbf{E}_e) = \int \frac{d\{x\}\, d\{p\}}{h^{5N}} e^{-\beta H(\{p\},\{x\},\mathbf{E},\mathbf{E}_e)}$$

In writing this equation the following have been used:

(a) h is Planck's constant.

(b) $\beta = 1/kT$, where k is the Boltzmann constant and T is the absolute temperature.

(c) The infinitesimal elements of integration have the following interpretation:

$$d\{x\} \equiv \prod_{i=1}^{N} d\mathbf{r}_i\, d\omega_i \equiv \prod_{i=1}^{N} d\mathbf{r}_i\, d\theta_i\, d\gamma_i$$

$$d\{p\} \equiv \prod_{i=1}^{N} d\mathbf{p}_i\, d\mathbf{L}_i \equiv \prod_{i=1}^{N} d\mathbf{p}_i\, dL_{\theta i}\, dL_{\gamma i}$$

The integrations over the center of mass variables, $\mathbf{r}_i$, are limited to the volume of the nanopore; the limits of the polar angles are, as usual, $0 \le \theta_i \le \pi$ and $0 \le \gamma_i \le 2\pi$, and the limits of the momentum variable components (both the linear and the angular momenta) are over all possible values, thus, for example, $-\infty \le p_{xi} \le \infty$ and $-\infty \le L_{\theta i} \le \infty$. Substituting the explicit form of the Hamiltonian from eq 5, the integrations over all the momentum variables yield:

$$Q(N,V,T,\mathbf{E},\mathbf{E}_e) = \frac{(2\pi IkT)^N (2\pi mkT)^{3N/2}}{h^{5N}} q_N(\mathbf{E},\mathbf{E}_e) \quad (7)$$

where we have

$$q_N(\mathbf{E},\mathbf{E}_e) \equiv \int \prod_{i=1}^{N} d\mathbf{r}_i\, d\omega_i \sin\theta_i D_N(\{x\},\mathbf{E},\mathbf{E}_e) \quad (8)$$

and

$$D_N(\{x\},\mathbf{E},\mathbf{E}_e) \equiv e^{-\beta[(\epsilon_0/2)\vartheta\Sigma_{i=1}^{N} E^2(\mathbf{r}_i) + U_N(\{x\},\mathbf{E},\mathbf{E}_e)]} \quad (9)$$

Henceforth, the factor $\sin\theta_i$ will be incorporated within the definition of $d\omega_i$ so that eq 8 may be written as

$$q_N(\mathbf{E},\mathbf{E}_e) \equiv \int d\{x\} D_N(\{x\},\mathbf{E},\mathbf{E}_e) \quad (10)$$

If the function $D_N(\{x\},\mathbf{E},\mathbf{E}_e)$ is divided by $q_N(\mathbf{E},\mathbf{E}_e)$, then the resulting function is the full N-body distribution function, $n_N(\{x\},\mathbf{E},\mathbf{E}_e)$, which will play an important role in the further development being presented in this paper:

$$n_N(\{x\},\mathbf{E},\mathbf{E}_e) = \frac{1}{q_N} D_N(\{x\},\mathbf{E},\mathbf{E}_e) \quad (11)$$

With use of eq 6, this distribution function becomes

$$n_N(\{x\},\mathbf{E},\mathbf{E}_e) = \frac{1}{q_N}\prod_{i=1}^{N} z^*(x_i) e^{-\beta\sum_{i<j}^{N} \psi(x_i,x_j)} \quad (12)$$

where

$$z^*(x_i) \equiv e^{-\beta\phi(x_i)} \quad (13)$$

From the full N-body distribution function, reduced generic m-body distribution functions, where $m < N$, are obtained by integration over $N - m$ variables

$$n_m(x_1,x_2,...x_m,\mathbf{E},\mathbf{E}_e) = \frac{N!}{(N-m)!}\int dx_{m+1}\, dx_{m+2} \ldots dx_N n_N(\{x\},\mathbf{E},\mathbf{E}_e) \quad (14)$$

Equations similar to (11) through (14) hold if either or both of the fields ($\mathbf{E}$ and $\mathbf{E}_e$) are absent. In the absence of either or both of these fields the terms that contain the relevant field/fields in the Hamiltonian will, of course, vanish.

In view of the integration of the momentum variables, the various functions that appear from now on will depend only on the spatial variables $x_1,x_2,$ .... It is expedient to introduce a further notational contraction whereby the spatial variable x_i is replaced by its subscript i. Thus, as an example, we may write

$$n_m(1,2,...,m) \equiv n_m(x_1,x_2,...,x_m)$$

(6) The Helmholtz free energy follows from the partition function:

$$A(\mathbf{E},\mathbf{E}_e) = -\beta^{-1} \ln Q(N,V,T,\mathbf{E},\mathbf{E}_e) = A^{ideal} + A^{excess}(\mathbf{E},\mathbf{E}_e) \quad (15)$$

where

$$A^{\text{ideal}} \equiv -\beta^{-1} \ln\left[\frac{(2\pi IkT)^N (2\pi mkT)^{3N/2}}{h^{5N}}\right]$$

$$A^{\text{excess}}(\mathbf{E},\mathbf{E}_e) \equiv -\beta^{-1} \ln q_N(\mathbf{E},\mathbf{E}_e)$$

(7) The polarization is given by the functional derivative of the Helmholtz free energy with respect to the external field:

$$\mathbf{P}(\mathbf{r},\mathbf{E},\mathbf{E}_e) = -\frac{\delta A(\mathbf{E},\mathbf{E}_e)}{\delta \mathbf{E}_e} \tag{16}$$

(8) As discussed in our earlier paper[41] the well-known relation relates the permittivity to the polarization:

$$\epsilon(\mathbf{E},\mathbf{E}_e) = n^2 + \frac{4\pi P(\mathbf{E},\mathbf{E}_e)}{\epsilon_0 E} \tag{17}$$

where n is the refractive index of the water; E and P are the magnitudes of the electric field ($\mathbf{E}$) and polarization ($\mathbf{P}$), respectively.

Permittivity Calculation. The permittivity is a quantity that is defined within the framework of a linear response theory, which implies that the system is perturbed by a weak perturbation such that the perturbed state can be expressed as a quantity that is, at most, linear in the perturbation. In the present analysis the weak perturbation is the external field, $\mathbf{E}_e$. To ensure that the computations are, indeed, being executed within a linear response framework, a functional Taylor expansion of the polarization in the external field is carried out and only the linear terms retained:

$$\mathbf{P}(\mathbf{r},\mathbf{E},\mathbf{E}_e) \simeq \int d\omega_1 n_1(\mathbf{r},\omega_1,\mathbf{E})\, \mu(\omega_1)\, \mu(\omega_1) + \beta \int d\omega_1\, n_1(\mathbf{r},\omega_1,\mathbf{E})\, \mu(\omega_1)\, \mu(\omega_1)\cdot\mathbf{E}_e(\mathbf{r}) + \beta \int d\mathbf{r}_1\, d\omega_1\, d\omega_2 h(\mathbf{r},\omega_1,\mathbf{r}_1,\omega_2,\mathbf{E})\, \mu(\omega_1)\, \mu(\omega_2)\cdot\mathbf{E}_e(\mathbf{r}) \tag{18}$$

In the present paper we will only consider the term of order zero in $\mathbf{E}_e$, not only because it is the simplest term but also because it is investigated in traditional calculations. A new function $h(\mathbf{r},\omega,\omega_1,\mathbf{E})$ called the *total correlation function* has appeared as a consequence of the functional differentiation, but it is related to the one- and two-body distribution functions defined in eq 14 in the following manner:

$$n_2(1,2,\mathbf{E}) = n_1(1,\mathbf{E})\, n_1(2,\mathbf{E})\, [h(1,2,\mathbf{E}) + 1] \tag{19}$$

The physical significance of the total correlation function can best be interpreted in terms of its well-known diagrammatic representation. In the absence of the intermolecular potential, $\psi(i,j)$, the function h vanishes.

Using eq 14 the one-body distribution function $n_1(1,\mathbf{E})$ can be written in terms of the two-body distribution function:

$$n_1(1,\mathbf{E}) = \frac{1}{(N-1)} \int d2 n_1(1,2,\mathbf{E})$$

This equation, along with eq 19, presents us with the possibility of writing an approximate form for $n_1(1,\mathbf{E})$ composed of two terms: one of which is entirely free of the intermolecular potential, $\psi(i,j)$:

$$n_2(1,2,\mathbf{E}) \simeq n_1^{(0)}(1,\mathbf{E})\, n_1^{(0)}(2,\mathbf{E})[h(1,2,\mathbf{E}) + 1] \tag{20}$$

Here

$$n_1^{(0)}(i,\mathbf{E}) = \frac{N}{q_1} e^{-\beta[\vartheta(\epsilon_0/2)E^2(\mathbf{r}_i) - \mu(\omega_i)\cdot\mathbf{E}(\mathbf{r}_i)]} \tag{21}$$

$$q_1(\mathbf{E}) = \int d\mathbf{r}\, d\omega\, e^{-\beta[\vartheta(\epsilon_0/2)E^2(\mathbf{r}) - \mu(\omega)\cdot\mathbf{E}(\mathbf{r})]} = \int d\mathbf{r}\, e^{-\beta\vartheta(\epsilon_0/2)E^2(\mathbf{r})} \frac{4\pi \sinh[\beta\mu E(\mathbf{r})]}{\beta\mu E(\mathbf{r})} \tag{22}$$

In writing the final form for q_1, the integrations over the angular variables have been carried out. Substitution of eq 20 in the first term of eq 18 yields

$$\mathbf{P}(\mathbf{r}) = \int d\omega_1\, \mu(\omega_1)\, n_1^{(0)}(\mathbf{r},\omega_1) + \frac{1}{N-1} \int d\omega_1\, d\mathbf{r}_1\, d\omega_2 \mu(\omega_1)\, n_1^{(0)}(\mathbf{r},\omega_1)\, n_1^{(0)}(\mathbf{r}_1,\omega_2)\, h(\mathbf{r},\omega_1,\mathbf{r}_1,\omega_2) \equiv \mathbf{P}_F(\mathbf{r}) + \mathbf{P}_{\text{corr}}(\mathbf{r}) \tag{23}$$

Because the angular integration in the first term of eq 23 can be carried out analytically we obtain

$$\mathbf{P}(\mathbf{r}) = \frac{4\pi N}{\beta q_1} e^{-\beta\vartheta(\epsilon_0/2)E^2(\mathbf{r})} \times \left[\frac{\cosh[\beta\mu E(\mathbf{r})]}{E^2(\mathbf{r})} - \frac{\sinh[\beta\mu E(\mathbf{r})]}{\beta\mu E^3(\mathbf{r})}\right]\mathbf{E}(\mathbf{r}) + \mathbf{P}_{\text{corr}}(\mathbf{r}) \tag{24}$$

The contribution of $\mathbf{P}_{\text{corr}}$ to the polarization due to the molecular correlation can be calculated once the total correlation function h has been computed. It can be readily shown that h satisfies the well-known Ornstein−Zernicke and this integral equation holds even within our nanopore system. This feature is demonstrated as follows:

(1) From eqs 10−13 it follows that

$$z^*(2)\frac{\delta n_1(1)}{\delta z^*(2)} \equiv \frac{\delta n_1(1)}{\delta \ln z^*(2)} = n_1(1)\, \delta(1,2) + n_1(1)\, n_1(2)\, h(1,2) \tag{25}$$

here $\delta(1,2)$ is the Dirac delta function.

(2) The *direct correlation* function, $c(1,2)$, is defined by

$$c(1,2) \equiv \frac{\delta \ln[n_1(1)/z^*(1)]}{\delta n_1(2)} = \frac{1}{n_1(1)}\delta(1,2) - \frac{\delta \ln z^*(1)}{\delta n_1(2)} \tag{26}$$

(3) Equation 25 provides the inverse of eq 26 and the two may be combined to yield the Ornstein−Zernicke equation:

$$h(1,2) = c(1,2) + \int d\bar{1} c(1,\bar{1})\, n_1(\bar{1})\, h(\bar{1},2)$$

Unfortunately, because a nanopore does not provide a translationally invariant environment, it is not possible to convert the Ornstein−Zernicke integral equation to an algebraic equation and thus obtain exact solutions. Moreover, because of the confinement of the water in the nanopore, the customarily used cluster expansion methods do not provide convergent series. In calculations involving bulk water it is generally assumed that the main contribution to any thermodynamic quantity comes from molecules that are separated by a macroscopic distance from each other; thus diagrams with small number of bonds (i.e., star diagrams) play a dominant role. In the present case we are denied such a macroscopic parameter and all diagrams make comparable contributions. Recently, Paul and Paddison[42] developed a variational approach that would provide analytic

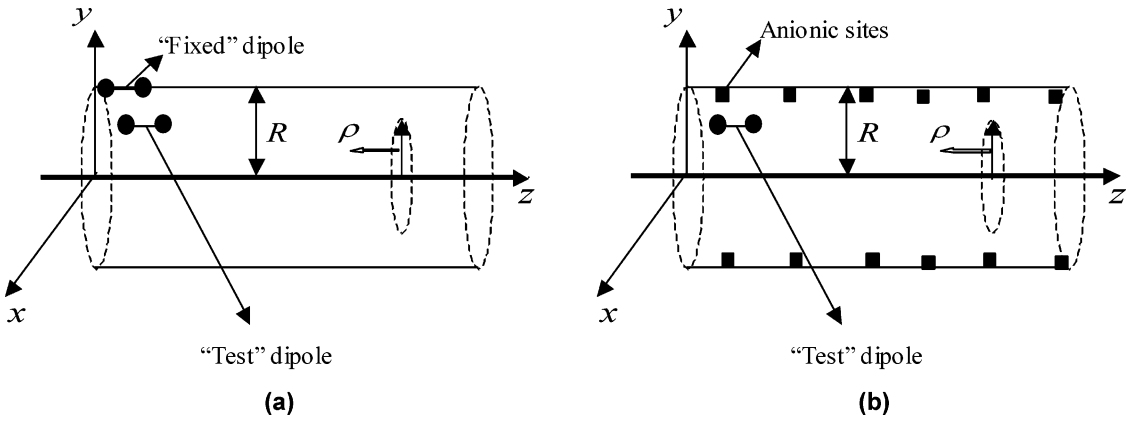

Figure 2. Pictorial representations of a membrane pore showing the methodology in computing the potentials due to interaction of the water dipoles with the internal field including both hard-core and dipolar interactions. In (a) the anionic sites (treated as point charges) are removed from the pore and only the "fixed" and the "test" dipoles are present. In (b) a similar treatment is considered but with the anionic sites included.

approximate solutions for the Ornstein−Zernicke equation and thus furnish a means for computing $\mathbf{P}_{corr}$. In the present work, however, we will assume that the internal field **E** is strong enough so that the interaction of the water dipoles with this field is greater than the intermolecular interaction. Under these conditions the polarization $\mathbf{P}_F$ will be the dominant term in eq 23. In the next section we make a comparison of these two interactions to provide some bounds to the validity of the assumption: $\mathbf{P}_F > \mathbf{P}_{corr}$.

Approximate Comparison of the Internal Field-Dipole Interactions with the Dipolar Interactions of the Water Molecules. For the purposes of this comparison we assume that the potential describing the interaction between the water molecules, $\psi(i,j)$, has the following form:

(a) A hard-core interaction, υ_s:

$$\upsilon_s(\mathbf{r}_i,\omega_i,\mathbf{r}_j,\omega_j) = \upsilon_s(|\mathbf{r}_i - \mathbf{r}_j|) = 0 \qquad |\mathbf{r}_i - \mathbf{r}_j| > \sigma$$
$$= \infty \qquad |\mathbf{r}_i - \mathbf{r}_j| < \sigma$$

(b) A dipolar interaction, υ_{dd}:

$$\upsilon_{dd} = \frac{1}{\epsilon_0}\mu(\omega_i)\cdot\overleftrightarrow{T}\cdot\mu(\omega_j)$$

$$\overleftrightarrow{T} = \frac{3(\mathbf{r}_i - \mathbf{r}_j)(\mathbf{r}_i - \mathbf{r}_j)}{|\mathbf{r}_i - \mathbf{r}_j|^5} - \frac{\overleftrightarrow{1}}{|\mathbf{r}_i - \mathbf{r}_j|^3}$$

Here, σ is the radius of the hard core and $\overleftrightarrow{1}$ is the unit tensor. As alluded to above, the interaction of the dipole with the internal field is given by $-\mu\cdot\mathbf{E}$.

With the interactions as defined above, we consider the following two situations, pictorially depicted in Figure 2:

(1) The anionic sites are removed from the nanopore, and a dipole hereafter referred to as the "*fixed*" dipole, is attached to the pore wall such that its axis lies parallel to the pore axis (see Figure 2a). The dipole may be placed anywhere along the pore length, but it is most conveniently located at $z = 0$. A second dipole, which we will refer to as a "test" dipole, is now introduced to compute the potential energy. There are a variety of orientations that can be used for the "test" dipole, our objective, however, is to examine the maximum value of the interaction potential to discover the conditions under which $\max|\psi| \leq |\mathbf{E}\cdot\mu|$. To achieve this, we examine the interaction maintaining the dipolar axis parallel to each other and move the test dipole along the cylindrical coordinates ρ and z. For such an orientation, the long-range component, υ_{dd}, takes the following form:

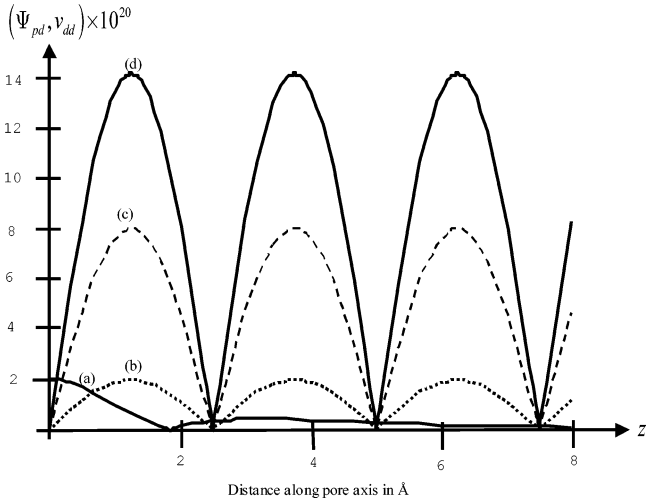

Figure 3. Plots of the potential experienced by the "test" dipole due to interaction with the internal field along the axial length of a typical Nafion membrane pore with hydration of 6 H_2O/SO_3 (where the radius and length of pore are 8 and 30 Å, respectively) for differential radial positions of the "test" and "fixed" dipoles. The reader is referred to the text for specific details of (a)−(d).

$$\upsilon_{dd}(\rho,z) = \frac{\mu^2[(R-\rho)^2 - 2z^2]}{4\pi\epsilon_0[(R-\rho)^2 + z^2]^{5/2}}$$

(2) The nanopore with its anionic charges intact (see Figure 2b) is considered with the same "test" dipole as in the previous case. For such a geometry, the interaction potential assumes the relatively simple form:

$$\Psi_{pd}(\rho,z) \equiv |\mu\cdot\mathbf{E}| = \left|\frac{2ef_n n^2\mu}{L^2\epsilon_0}K_1\left[\frac{2n\pi(R-\rho)}{L}\right]\sin\left[\frac{2n\pi z}{L}\right]\right|$$

In Figure 3 we show four plots (labeled (a) through (d)) that compare the potentials experienced by the "test" dipole. For the purposes of these calculations we have taken an average pore found in a Nafion membrane with a hydration level of six water molecules per SO_3^- group (i.e., $\lambda = 6$). The radius (R) and length (L) of such a pore are 8 and 30 Å, respectively. The values of the other pertinent parameters are $n = 6$ and $f_n = 6$.

In Figure 3a the "test" dipole has been placed at a distance of 2.6 Å from the pore wall. Therefore, at $z = 0$ the distance between the centers of the "fixed" and "test" dipoles is 2.6 Å.

It follows therefore, that given the relative orientation of the two dipoles, the value of υ_{dd} at this point will have the maximum value that it can acquire in the pore. The rest of the curve corresponds to the variation in the potential as the "test" dipole is moved along the *z*-axis maintaining its initial orientation. We do not move the "test" dipole over the entire pore length of 30 Å but only to a distance of 8 Å, which is sufficient for the present calculation. In Figure 3b the same calculation is repeated but with the "fixed" dipole replaced by the anionic sites. However, the test dipole has been placed at a distance of 4 Å from the pore wall (that is, half the radius of the pore). It is evident that at this distance from the anionic sites the interaction between two water molecules is comparable with the interaction between the internal field and the water molecules. In Figure 3c the "test" dipole has been placed at a distance of 3 Å from the pore wall. Here the interaction between the internal field and the dipole is larger, except at the nodal points where $\Psi_{pd} = 0$. Finally, in Figure 3d the "test" dipole has been placed at a distance of 2.6 Å from the pore wall (anionic sites) and it is clear that here the internal field-dipole interaction is the dominant one.

The conclusions from this analysis may be summarized as follows:

(1) If we assume the completely hypothetical picture in which all the water molecules are present as nearest neighbors, then the interaction between the internal field and the water dipoles will be weaker than the dipole−dipole interactions beyond a distance of approximately half the radius of the pore.

(2) The water molecules that are present close to the center of the pore are sufficiently well removed from the anionic sites that they may be treated as bulk water with similar thermodynamic properties.

(3) The assumption $\mathbf{P}_F > \mathbf{P}_{corr}$ is reasonable if it is augmented with the requirement that at the pore axis all physical properties are given values corresponding to bulk water.

Calculation of the Permittivity without the Intermolecular Interactions. Neglecting the polarization term, $\mathbf{P}_{corr}$, in eq 24, we substitute the remainder into eq 17 to obtain a spatially dependent permittivity given by

$$\epsilon(\mathbf{r}) = n^2 + \frac{16\pi^2 N}{\beta\epsilon_0 E^2(\mathbf{r}) q_1} e^{-\beta\vartheta(\epsilon_0/2)E^2(\mathbf{r})}\left[\coth\{\beta\mu E(\mathbf{r})\} - \frac{1}{\beta\mu E(\mathbf{r})}\right]\sinh\{\beta\mu E(\mathbf{r})\} \quad (27)$$

Equation 27 is a new expression for the permittivity and becomes identical to the traditional expressions if the energy of the internal field is neglected (achieved by allowing $\vartheta \rightarrow 0$). One of the most important features of this new result is that it does not diverge in close proximity to the anionic sites. This is in contrast to the traditional expressions that diverge when $\vartheta \rightarrow 0$, unless it is assumed that either **E** is a constant or a slowly varying function of the spatial variable. Under either of these two assumptions, all **E** dependent quantities can be removed from the spatial integral involved in q_1 (see eq 22) and these functions of **E** will ensure convergence of $\epsilon(\mathbf{r})$ close to the anionic sites.

Results and Discussion

As shown in the previous section, the pore interior may be approximately partitioned into two regions:

(1) A region in close proximity to the pore axis: here the affects of the internal field are minimal and the intermolecular forces determine the properties of the water, thus the permittivity is approximately that of bulk water.

(2) A region in close proximity to the ionic sites: here the intensity of the internal field is greatest, a fall in the permittivity (i.e., dielectric saturation) is expected.

It is evident that the volumes of these two regions will depend critically upon the structural properties of the pore; consequently we define a volume fraction, V_F, in the following manner:

$$V_F(\lambda) = \frac{V_B}{V} \times 100 \quad (28)$$

Here, λ is the degree of hydration of the membrane as measured by the number of water molecules per $-SO_3^-$ group, V_B is the volume of water in the pore that possesses the same permittivity as bulk water, and V is the total volume of the pore. Clearly, the pore morphology is reflected in the value of V_F, as discussed above. Equation 27 is a space dependent expression for the permittivity. Now as long as the permittivity becomes equal to that of bulk water at very large distances from the anionic sites, this equation may be used as a means of computed the radial dependence of the permittivity and V_F.

The structural features that influence both a plot of the permittivity as a function of radial distance from the pore axis and the volume fraction are as follows:

(1) The length, *p*, of protrusion of the $-SO_3^-$ groups into the pore interior.

(2) The number of axially positioned rings, *n*, over which a fixed number of $-SO_3^-$ groups are distributed.

To begin with, we use our new result of eq 27 to recalculate radial cross sections of the water permittivity in both Nafion and PEEKK membrane pores over a range of water contents specified by the value of the parameter λ. The relevant structural information for these membranes is summarized in Table 1.

TABLE 1: Pore Parameters for Nafion and 65 % Sulfonated PEEKK Membranes

parameter	Nafion			PEEKK		
λ	6	13	22.5	15	23	30
L, Å	30	56	64	40	48	56
n	6	8	8	5	6	7
N	216	1001	1800	375	828	1470
R, Å	8	14	16	7	9.5	12
intrusion, *p* Å	4	4	4	1	1	1
f_n	6	9.5	10	5	6	7

Now before the data from Table 1 can be substituted into eq 27, the quantity q_1 (defined in eq 22) must first be computed by numerical integration resulting in q_1 as a parameter in the expression. In our work, however, we do not carry out this integration but compute q_1 such that when the permittivity is calculated at a large distance from the anionic sites, it acquires a value equal to that of bulk water, taken to be 80. Such an approach immediately guarantees that the dominant interaction in this region is the intermolecular interactions between the water molecules as required by the calculations presented in the previous section. In calculating the permittivity, the radial distance, ρ, measured from the pore axis, is allowed to increase until a distance of 1 Å from an anionic group (located at a distance *p* from the pore wall) is reached. This break is needed because the internal field diverges at the anionic site. In general, the calculation may once again be commenced after another break of 1 Å past the anionic site has been made and the calculation continued to the pore wall. It is not obvious, however, that this is the correct approach to adopt because this region contains chains of the backbone material, which are

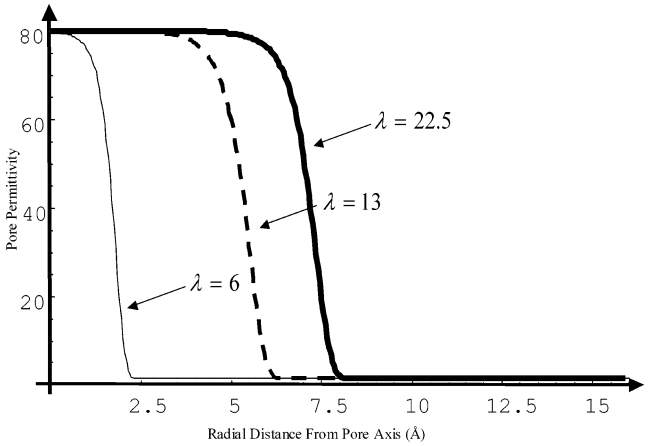

Figure 4. Radial dependence of the permittivity (i.e., dielectric constant) of water in Nafion membrane pores at degrees of hydration of 6, 13, and 22.5 H_2O/SO_3. In all cases the dielectric constant falls from a value of 80 in the center of the pore to a value of approximately 2 (that of the polymer backbone). The plots show that at 13 and 22.5 H_2O/SO_3 there is fraction of "bulklike" water in the pore.

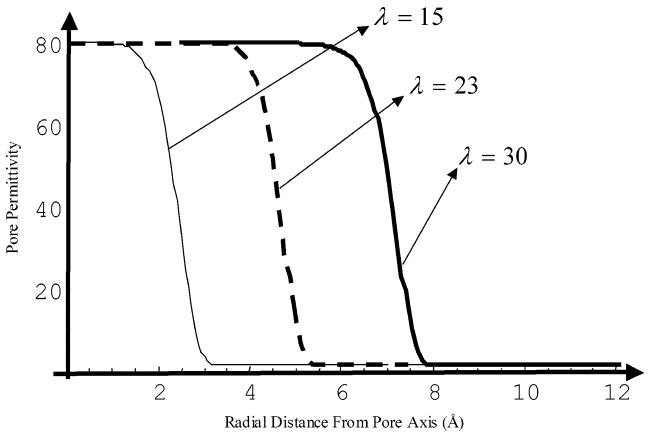

Figure 5. Dielectric constant of the water in PEEKK membrane pores plotted as a function of the distance from the center of the pore for various degrees of hydration (i.e., 15, 23, and 30 H_2O/SO_3). The volume fraction of "bulklike" water increases substantially over the range of hydration.

absent in the region before the first break. In our calculations we stop at the first break and assume that the rest of pore has the permittivity approximately equal to this value. The permittivity is computed along the entire length of the pore at equally spaced intervals of 1 Å and subsequently averaged.

Plots of radial cross-sections in the water permittivity for both Nafion and 65% sulfonated PEEKK membranes over a range of hydration levels are presented in Figures 4 and 5, respectively. All plots show the expected decrease in the dielectric constant as the pore wall (and anionic sites) is approached; and an increase in a central region surrounding the pore axis possessing the dielectric constant of bulk water (i.e., 80). Although these results with our new formulation (i.e., eq 27) are qualitatively similar to our previous results,[41] there are some important differences and improvements. A greater distinction is now observed in the volume of "bulklike" water as the degree of hydration is increased in the PEEKK membranes (i.e., as λ is increased from 15 to 30). This result is in better agreement with the increase observed in the proton self-diffusion coefficients as measured by pulsed field gradient NMR experiments.[7] The main differences in the quantitative details can be appreciated by reference to eq 27, which gives the permittivity as a function of space, **r**, and the quantity $q_1(\mathbf{E})$ defined in eq 22.

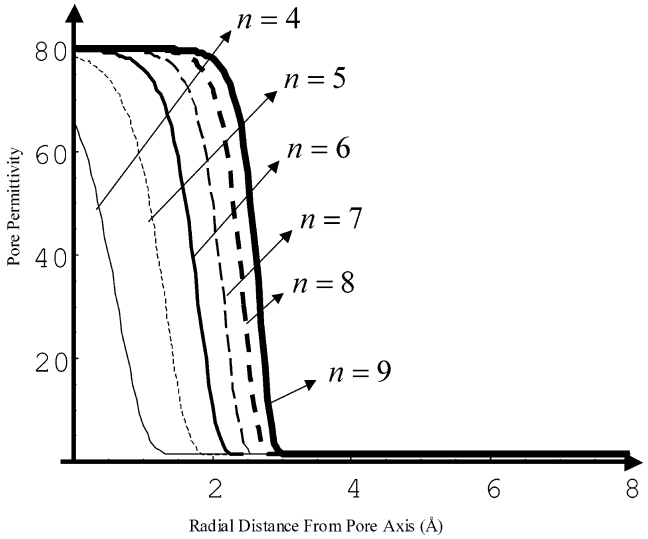

Figure 6. Plots of the radial dependence in the water permittivity for a hypothetical membrane pore with fixed water content, total number of anionic sites, and pore dimensions but with various distributions of the fixed anionic sites. The distribution of the fixed sites is varied from a completely homogeneous distribution when $n = 9$ to a very inhomogeneous distribution when $n = 4$ (i.e., where there are areas within the pore where the anionic density is high separated by regions where it is very low). The results show that the volume fraction of bulklike water can be increased from 0 to as high as 6%.

The following steps recover our previous work:[41] (1) setting $\vartheta = 0$ in eq 27 and (2) assuming that the field $\mathbf{E}(\mathbf{r})$ is a slowly varying function of **r** so that it may be removed from the integrand defining q_1. It is a consequence of the latter that results in the appearance of $\mathbf{E}(\mathbf{r})$ in the denominator of $\epsilon(\mathbf{r})$, derived in our previous work. The permittivity falls in the neighborhood of the anionic sites due to the rise of this field intensity. In the present work, however, the drop in the permittivity is due to the Gaussian field dependent factor in $\epsilon(\mathbf{r})$ and therefore differences appear in the curvature of the plots in the proximity of the anions. The present work, therefore, does not require the unreasonable assumption of a weak spatially dependent field.

As a means of assessing the affects of different anionic charge densities and distributions on the permittivity of the water, the number of radially symmetric arrays (i.e., rings) of $-SO_3^-$ groups was varied while the total amount of charge was kept fixed in a hypothetical membrane pore with water content and pore dimensions similar to Nafion with $\lambda = 6$ (see Table 1). The number of these rings was varied from $n = 4$, corresponding to a very inhomogeneous distribution of sulfonate groups along the length of the pore with local regions of high anionic charge density (i.e., aggregation of the sulfonate groups), to $n = 9$, where the charge is uniformly (i.e., smoothly) distributed within the pore. Radial cross sections of the dielectric constant of the water are plotted for the various charge distributions in Figure 6. These plots clearly demonstrate that by only increasing the uniformity in the sulfonate distribution, the ordering and dielectric saturation of the water can be substantially decreased from pores showing no "free" or "bulklike water" (i.e., for $n = 4-6$) to pores with as much as 6% (see eq 28). With transport of protons a function of the state of the water, these calculations, in agreement with our proton diffusion calculations,[21] attest to the fact that local density and distribution of the fixed sites within a PEM strongly influence proton conduction in the membrane.

In a second investigation we studied the affects of changing the length of intrusion of the fixed sites within the membrane

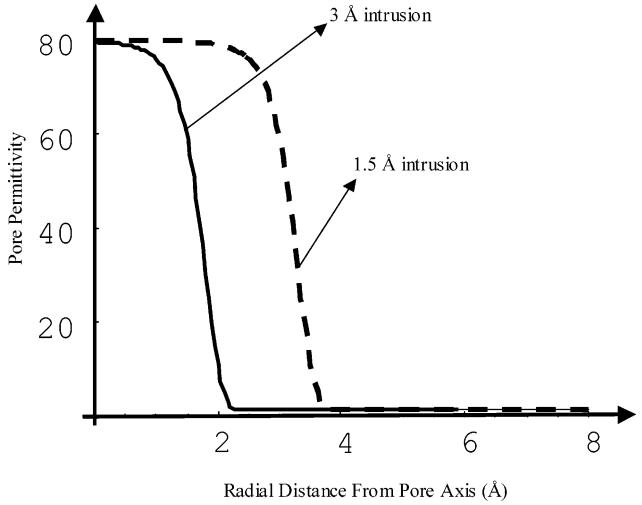

Figure 7. Effects of increasing the intrusion of the anionic groups from a distance from the pore wall of 1.5−3.0 Å in a Nafion type membrane pore with fixed water content (i.e., $\lambda = 6$); dimensions, and SO_3^- distribution. Clearly, the fraction of "bulk water" increases as the intrusion of the sulfonate groups is decreased.

pore on the dielectric response of the water. This was motivated by the observed differences in the transport properties of PEMs with distinct side chains (i.e., length and chemistry). Similar to the previous study, the calculations were conducted in a pore with fixed dimensions and constant total number of sulfonate groups (as found in Nafion membranes with a water content of 6 H_2Os/SO_3^-). The distribution of the sulfonate groups was also not changed. The permittivity of the water as a function of radial position is plotted for pores where the anionic groups are 3.0 and 1.5 Å from the pore wall and displayed in Figure 7. These results show that as the anionic sites penetrate further into the pore interior, they are brought into closer proximity to the region where "bulklike" water persists, leading to a more dramatic display of dielectric saturation. It is also interesting to witness the affects of what might be perceived as only a slight or insignificant change in side chain length (i.e., an intrusion increase of only 1.5 Å) to the nature of the water. These results indicate the importance of structural features of the polymer on the transport properties of the material.

As has been discussed in the introductory section of this paper, the permittivity of the water in the membrane is one of several macroscopic properties that play an important role in determining the transport of protons in the membrane. It is the water permittivity that modulates the strength of the interactions between the transported protons[7] and the internal field. At the same time, the permittivity is itself a function of the internal field. We have shown, however, that the latter is a consequence of the basic morphological characteristics of the nanopore and therefore these structural features are manifested as deviations in the permittivity of water contained in the pore from its value in bulk water.

Conclusions

In this paper we have refined a molecular statistical mechanical model for the computation of the spatially dependent water permittivity in the pores of hydrated polymer electrolyte membranes. The principal motivation for this improvement is the fact that in the traditional models the internal electrical fields, arising from the ionization of the sulfonic acid groups, are treated as the external fields in bulk calculations resulting in nonphysical divergence of the permittivity. We have included the energy of the internal field as a term in the Hamiltonian, which eliminates the divergent behavior, and the permittivity thus computed exhibits an appropriate dielectric saturation phenomenon in regions where the field is strong.

The anionic sites are fixed to the pendant chains whereas their counterions, the hydronium ions, being mobile, are more evenly distributed; thus the electrical field between these charged species is nonhomogeneous. From this distribution it is evident that the field will be more intense close to the anionic sites. We have shown, by using simple model calculations involving dipoles, that close to the anionic sites the interaction of the electrical field with the dipoles is stronger than the interactions between the dipoles. Therefore, it is reasonable to compute the polarization and the permittivity by neglecting the dipole/dipole interactions. Far from the anionic sites we assume that the water molecules behave like bulk water. Although our simply model has neglected the confinement effects due to the hydrophobic interaction of the water with the polymer backbone, these affects are considerably smaller than the effects of the interaction of the sulfonate groups with the water. Due to the fact that the nature (size, distribution, etc.) of the water domains is to a large extent controlled by the density and distribution of the anionic groups, this confinement effect has been implicitly included in our model. Our calculations show that even over the distance of several angstroms (i.e., across the radius of a membrane pore) substantial screening of the sulfonate groups does occur. This screening (i.e., dielectric saturation) will result in substantially different distribution of the mobile protons in the pore than would be predicted by a Boltzmann distribution.

Because the pendant groups are features that are characteristic of the pore morphology it is reasonable to expect that the permittivity should be a useful indicator of the pore morphology. We have confirmed this prediction by calculating the fraction of water in the pore that has bulklike properties as a function of (1) the "smoothness" with which the anionic charge is distributed over the pendant groups and (2) the length of the pendant group penetration into the pore volume. It is clear that as the same amount of charge is spread over a larger number of pendant groups the field will tend toward a greater degree of homogeneity reducing, thereby, the degree of dielectric saturation: a fact that is born out by the enhancement in the fraction of bulklike water. The increase in the pendant chain length places the anionic sites more deeply into the bulk water region of the pore causing depletion in the fraction of total bulk water within the pore.

Acknowledgment. R.P. gratefully acknowledges support from the Natural Sciences and Engineering Research Council of Canada (NSERC).

Appendix

The contribution of the internal field to the Hamiltonian may be estimated in the following manner:

(1) We consider the nanopore to contain M pendant groups, attached to the pore wall, each carrying a single $-SO_3^-$ anion and M H_3O^+ ions that are free to move within the pore volume. In Figure 8 only a single representative pendant group, j, and a single representative H_3O^+ ion, k, are shown.

(2) Let the location of the representative anion and cation be denoted by the vectors $\mathbf{r}_{ja}$ and $\mathbf{r}_{kc}$, respectively. These vectors are drawn from the origin of a space fixed coordinate frame to the centers of the volumes, $V(\mathbf{r}_{ja})$ and $V(\mathbf{r}_{kc})$, occupied by each of the two ions.

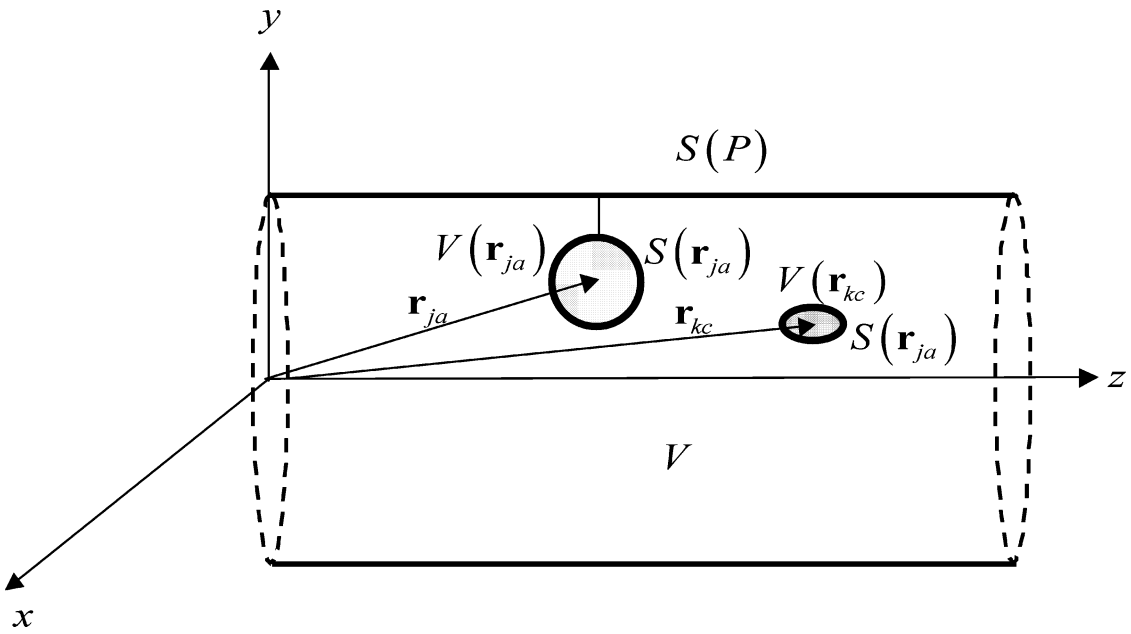

Figure 8. Sign convention used in the computation of the internal field energy where the position of an anionic fixed site and conjugate hydrated proton is denoted $\mathbf{r}_{ja}$ and $\mathbf{r}_{kc}$, respectively; and the associated volumes $V(\mathbf{r}_{ja})$ and $V(\mathbf{r}_{kc})$. The reader is referred to the Appendix for complete details.

(3) The total energy (internal field energy) due to the anions and the hydronium ions will be given by

$$U_{\mathrm{F}} = \sum_{j=1}^{M} \Psi(\mathbf{r}_{ja})\, Q(\mathbf{r}_{ja}) + \sum_{j=1}^{M} \Psi(\mathbf{r}_{jc})\, Q(\mathbf{r}_{jc})$$

In writing this equation we assume that the potential Ψ *is constant within each* of the ionic volumes and the charge symbol Q includes the appropriate sign of the charge.

(4) Using the fact that Gauss' law relates the charge densities $\rho(\mathbf{r}_{ja})$ and $\rho(\mathbf{r}_{jc})$ to the local displacement vectors: $\rho(\mathbf{r}_{ja}) = \nabla\cdot\mathbf{D}(\mathbf{r}_{ja})$ and $\rho(\mathbf{r}_{jc}) = \nabla\cdot\mathbf{D}(\mathbf{r}_{jc})$ the total energy may be expressed as

$$U_{\mathrm{F}} = \sum_{j=1}^{M} \Psi(\mathbf{r}_{ja}) \int_{V(\mathbf{r}_{ja})} \mathrm{d}\mathbf{r}\, \nabla\cdot\mathbf{D}(\mathbf{r}) + \sum_{j=1}^{M} \Psi(\mathbf{r}_{jc}) \int_{V(\mathbf{r}_{jc})} \mathrm{d}\mathbf{r}\, \nabla\cdot\mathbf{D}(\mathbf{r})$$

(5) Converting to surface integrals we obtain

$$U_{\mathrm{F}} = \sum_{j=1}^{M} \Psi(\mathbf{r}_{ja}) \int_{S(\mathbf{r}_{ja})} \mathrm{d}\mathbf{S}^{(\mathrm{o})}\cdot\mathbf{D}(\mathbf{r}\in S(\mathbf{r}_{ja})) + \sum_{j=1}^{M} \Psi(\mathbf{r}_{jc}) \int_{S(\mathbf{r}_{jc})} \mathrm{d}\mathbf{S}^{(\mathrm{o})}\cdot\mathbf{D}(\mathbf{r}\in S(\mathbf{r}_{jc}))$$

In keeping with the usual geometric convention, the surface vector $\mathrm{d}\mathbf{S}^{(\mathrm{o})}$ is a vector normal to the surface and points out of each ionic volume. It is useful to write this result in terms of the vector $\mathrm{d}\mathbf{S} = -\mathrm{d}\mathbf{S}^{(\mathrm{o})}$, which points into the interior of the ionic volumes:

$$U_{\mathrm{F}} = -\sum_{j=1}^{M} \Psi(\mathbf{r}_{ja}) \int_{S(\mathbf{r}_{ja})} \mathrm{d}\mathbf{S}\cdot\mathbf{D}(\mathbf{r}\in S(\mathbf{r}_{ja})) - \sum_{j=1}^{M} \Psi(\mathbf{r}_{jc}) \int_{S(\mathbf{r}_{jc})} \mathrm{d}\mathbf{S}\cdot\mathbf{D}(\mathbf{r}\in S(\mathbf{r}_{jc}))$$

(6) Let any function with the argument P denote the value of that function on the outer wall of the pore. Thus, $\Psi(P)$ would be the potential at the outer pore wall and $S(P)$ the area of the outer pore wall. If we assume that $\Psi(P) = 0$, then we must have

$$\Psi(P) \int_{S(P)} \mathrm{d}\mathbf{S}\cdot\mathbf{D}(\mathbf{r}\in S(P)) = 0$$

Adding this vanishing result to the previous expression for the energy, we obtain

$$U_{\mathrm{F}} = -\sum_{j=1}^{M} \Psi(\mathbf{r}_{ja}) \int_{S(\mathbf{r}_{ja})} \mathrm{d}\mathbf{S}\cdot\mathbf{D}(\mathbf{r}\in S(\mathbf{r}_{ja})) - \sum_{j=1}^{M} \Psi(\mathbf{r}_{jc}) \int_{S(\mathbf{r}_{jc})} \mathrm{d}\mathbf{S}\cdot\mathbf{D}(\mathbf{r}\in S(\mathbf{r}_{jc})) - \Psi(P) \int_{S(P)} \mathrm{d}\mathbf{S}\cdot\mathbf{D}(\mathbf{r}\in S(P))$$

(7) It is evident that, collectively, the surface in the above integrals is the total surface ∂V that encloses the volume V, which is the total volume of the pore less the volume occupied by all the ions. Thus, a compact expression for the energy may be written as

$$U_{\mathrm{F}} = -\int_{\partial V} \Psi(\mathbf{r}\in\partial\mathbf{V})\, \mathbf{D}(\mathbf{r}\in\partial\mathbf{V})\cdot\mathrm{d}\mathbf{S} = -\int_{V} \mathrm{d}\mathbf{r}\, \Psi(\mathbf{r})\nabla\cdot\mathbf{D}(\mathbf{r})$$

In writing this equation, it is necessary to include the potential Ψ within the integrand because it is a function that varies with the different surfaces involved in ∂V. The last member follows from an application of Gauss' law.

(8) If the charge density on the ion sites is changed by an amount $\delta\rho$ at a fixed potential, then in keeping with Gauss' law this will produce a change $\delta\mathbf{D}$ in the displacement vector and a change in energy given by

$$\delta U_{\mathrm{F}} = -\int_{V} \mathrm{d}\mathbf{r}\, \nabla\cdot[\Psi(\mathbf{r})\, \delta\mathbf{D}(\mathbf{r})] = -\int_{V} \mathrm{d}\mathbf{r}\, [\nabla\Psi(\mathbf{r})]\cdot\delta\mathbf{D}(\mathbf{r}) - \int_{V} \mathrm{d}\mathbf{r}\, \Psi(\mathbf{r})[\nabla\cdot\delta\mathbf{D}(\mathbf{r})]$$

The last term in this equation must vanish because, from Gauss' law, $\nabla\cdot\delta\mathbf{D}(\mathbf{r})$ corresponds to a charge density change. However, the variable $\mathbf{r}$ is restricted, by virtue of the integration limits, to the volume V where the ions, by definition, do not reside.

(9) From the definition of the field as the negative gradient of the potential: $\mathbf{E} = -\nabla\Psi$ and the definition of the displacement vector: $\mathbf{D} = \epsilon_0\mathbf{E}$, assuming vacuum in V, we obtain

$$\delta U_F = \epsilon_0 \int_V d\mathbf{r}\, \mathbf{E}\cdot\delta\mathbf{E} = \delta\left[\frac{\epsilon_0}{2}\int_V d\mathbf{r}\, E^2\right]$$

We obtain an expression for the energy due to the pendant groups and the hydronium ions in a vacuum of the form

$$U_F = \frac{\epsilon_0}{2}\int_V d\mathbf{r}\, E^2$$

(10) In the problem that concerns us in this paper we are interested in computing the permittivity of water within the pore. Let us assume that the pore contains N water molecules then each water molecule may be ascribed a volume:

$$\vartheta = \frac{V}{N}$$

Thus the integral in the above expression may be computed as a sum:

$$U_F = \frac{\epsilon_0}{2}\vartheta\sum_{i=1}^{N} E^2(\mathbf{r}_i) \qquad (29)$$

Here, $\mathbf{r}_i$ is a vector that locates the center of mass of the ith water molecule in a volume ϑ. The above energy due to the electrical field arising from the pendant and hydronium ions must be included in the Hamiltonian of the system.

References and Notes

(1) Steele, B. C. H.; Heinzel, A. *Nature* **2001**, *414*, 345.
(2) Kreuer, K. D. *ChemPhysChem* **2002**, *3*, 771.
(3) Doyle, M.; Rajendran, G. Perfluorinated membranes. In *Handbook of Fuel Cells − Fundamentals, Technology and Applications Volume 3 − Fuel Cell Technology and Applications*; Vielstich, W., Lamm, A., Gasteiger, H., Eds.; J. Wiley and Sons: Chichester, U.K., 2003.
(4) Kreuer, K. D. Hydrocarbon membranes. In *Handbook of Fuel Cells − Fundamentals, Technology and Applications Volume 3 − Fuel Cell Technology and Applications*; Vielstich, W., Lamm, A., Gasteiger, H., Eds.; J. Wiley and Sons: Chichester, U.K., 2003.
(5) Paddison, S. J. First principles modeling of sulfonic acid based ionomer membranes. In *Handbook of Fuel Cells − Fundamentals, Technology and Applications Volume 3 − Fuel Cell Technology and Applications*; Vielstich, W., Lamm, A., Gasteiger, H., Eds.; J. Wiley and Sons: Chichester, U.K., 2003.
(6) Paddison, S. J. *Annu. Rev. Mater. Res.* **2003**, *33*, 289.
(7) Kreuer, K. D. *J. Membr. Sci.* **2001**, *185*, 29.
(8) Belletete, M.; Lachapelle, M.; Durocher, G. *J. Phys. Chem.* **1990**, *94*, 5337.
(9) Ray, J. Guha; Sengupta, P. K. *Chem. Phys. Lett.* **1994**, *230*, 75.
(10) Das, K.; Sarkar, N.; Das, S.; Datta, A.; Bhattacharyya, K. *Chem. Phys. Lett.* **1996**, *249*, 323.
(11) Datta, A.; Mandal, D.; Pal, S. K.; Bhattacharyya, K. *J. Phys. Chem. B* **1997**, *101*, 10221.
(12) Faeder, J.; Ladanyi, B. M. *J. Chem. Phys.* **2000**, *104*, 1033.
(13) Roux, B.; Karplus, M. *Annu. Rev. Biophys. Biomol. Struct.* **1994**, *23*, 731.
(14) Breed, J.; Sankararamakrishnan, R.; Kerr, I. D.; Sansom, M. S. P. *Biophys. J.* **1996**, *70*, 1643.
(15) Senapati, S.; Chandra, A. *J. Phys. Chem. B* **2001**, *105*, 5106.
(16) Agmon, N. *Chem. Phys. Lett.* **1995**, *244*, 456.
(17) Tuckerman, M. E.; Marx, D.; Klein, M. L.; Parrinello, M. *Science* **1997**, *275*, 817.
(18) Kreuer, K. D. *Solid State Ionics* **2000**, *136−137*, 149.
(19) Hartnig, C.; Witschel, W.; Spohr, E. *J. Phys. Chem. B* **1998**, *102*, 1241.
(20) Paddison, S. J.; Paul, R.; Zawodzinski, T. A., Jr. *J. Electrochem. Soc.* **2000**, *147*, 617.
(21) Paddison, S. J.; Paul, R.; Zawodzinski, T. A., Jr. *J. Chem. Phys.* **2001**, *115*, 7753.
(22) Paddison S. J.; Paul, R. *Phys. Chem. Chem. Phys.* **2002**, *4*, 1158.
(23) Paddison, S. J.; Reagor, D. W.; Zawodzinski, T. A. *J. Electroanal. Chem.* **1998**, *459*, 91.
(24) Paddison, S. J.; Bender, G.; Kreuer, K. D.; Nicoloso, N.; Zawodzinski, T. A., Jr. *J. New Mater. Electrochem. Systems* **2000**, *3*, 291.
(25) MacMillan, B.; Sharp, A. R.; Armstrong, R. L. *Polymer* **1999**, *40*, 2471.
(26) Böttcher, C. J. F. *Theory of Electric Polarization*, 2nd ed.; Elsevier Scientific: Amsterdam, 1973.
(27) Kerr, J. *Philos. Mag.* **1875**, *50*, 337.
(28) Coffey, W. T.; Scaife, B. K. P. *J. Electrostatics* **1975**, *1*, 193.
(29) Paddison, S. J.; Paul, R.; Kaler, K. V. I. S. *Bioelectrochem. Bioener.* **1995**, *38*, 321.
(30) Kirkwood, J. G. *J. Chem. Phys.* **1936**, *4*, 592.
(31) Kirkwood, J. G. *J. Chem. Phys.* **1939**, *7*, 911.
(32) Fröhlich, H. *Trans. Faraday Soc.* **1948**, *44*, 238.
(33) Fröhlich, H. *Theory of Dielectrics; dielectric constant and dielectric loss*, 2nd ed; Clarendon Press: Oxford, U.K., 1958.
(34) Buckingham, A. D. *J. Chem. Phys.* **1956**, *25*, 428.
(35) Booth, F. *J. Chem. Phys.* **1950**, *19*, 391.
(36) Bontha, J. R.; Pintauro, P. N. *Chem. Eng. Sci.* **1994**, *49*, 3835.
(37) Nienhaus, G.; Deutch, J. M. *J. Chem. Phys.* **1972**, *56*, 1819.
(38) Warshel, A.; Papazyan, *Curr. Opin. Struct.* **1998**, *8*, 212.
(39) Sansom, M. S. P.; Smith, G. R.; Adcock, C. *Biophys. J.* **1997**, *73*, 2404.
(40) Paul, R.; Paddison, S. J. In *Advances in Materials Theory and Modeling − Bridging Over Multiple-Length and Time Scales*; Bulatov, V., Colombo, L., Cleri, F., Lewis, L. J., Mousseau, N., Eds.; Materials Research Society: Warrendale, PA, 2001.
(41) Paul, R.; Paddison, S. J. *J. Chem. Phys.* **2001**, *115*, 7762.
(42) Paul, R.; Paddison, S. J. *Phys. Rev. E* **2003**, *67*, 016108.